II International Conference on Particle-based Methods – Fundamentals and Applications
PARTICLES 2011
E. Oñate and D.R.J. Owen (Eds)

SCALING ANALYSIS OF DEFORMATION FIELD WITHIN GRANULAR MATERIALS: APPLICATION TO STRAIN LOCALIZATION

FLORENT GIMBERT*, GAEL COMBE†, DAVID AMITRANO* AND JEROME WEISS#

*Institut des Sciences de la Terre (ISTerre)
CNRS, Université Joseph Fourrier
Domaine Universitaire
38401 GENOBLE, France
e-mail: florent.gimbert@ujf-grenoble.fr

† Laboratoire Sols, Solides, Structures, Risques (3SR)
UMR 5521 (UJF, INPG, CNRS)
Domaine Universitaire
38041 GRENOBLE Cedex 9, France

#Laboratoire de Glaciologie et de Géophysique de l'Environnement (LGGE)
CNRS, Université Joseph Fourrier
38402 St Matin d'Hères, France

Key words: Strain Localization, Granular Materials, DEM, Long Range Correlations, Critical Behaviour.

Abstract. Discrete element method (DEM) simulations using periodic boundary conditions and molecular dynamics are conducted on a frictional granular media. Two dimensional strain controlled biaxial tests are carried out on an assembly of circular particles interacting via elastic contacts and Coulomb friction. The spatial correlations that take place within the deformation field along the loading path are tracked by a scaling analysis of the continuous strain rate field. This method allows us to discuss the degree of strain localization occurring throughout the test. The analysis of the correlation length in the early stages of macroscopic deformation leads to the identification of two distinct behaviors. First, a divergence of the correlation length on the first deformation invariant, i.e. the divergence, is reported at the onset of macroscopic dilation. This suggests an interpretation of the contraction peak as a critical point. Secondly, an increase of the correlation length on the second deformation invariant, i.e. the shear, is also observed before the peak load. However, saturation remains on the scaling law. We argue that this second behavior is associated to macroscopic shear banding: our analysis accurately gives its outbreak on the stress versus strain curve. Finally, a dependence of the correlation length as a function of the deformation window considered is reported. This shows that scaling properties within the deformation field emerge from long range interactions within an assembly of rigid frictional particles.

1 INTRODUCTION

Discrete element numerical simulations (DEM) of granular materials show an extraordinarily rich behavior emerging from simple mechanical interactions at the particle scale.

As shown by Radjai and Roux [1], a homogeneous macroscopic loading applied to a granular material constituted of a random assembly of rigid circular frictional particles leads to the development of large, non-gaussian particle velocity fluctuations at small time scales, as well as a power law decay of the spatial power spectrum of the velocity field. This indicates long-range correlations. Indeed, heterogeneous distribution of contact forces on scales much larger than the typical particle size [2-3] induces collective motions of particle assemblies, i.e. long range correlations, to operate within granular media. Thus, to characterize the mechanical fields (stress, strain) within granular materials from the particle scale to the large scale is of first interest in order to describe and understand properly their macroscopic mechanical response.

Following this route, the objective of this paper is to investigate the spatial correlations that take place within the deformation field of frictional granular materials during compressive loading. Can classical macroscopic features such as dilatancy or shear banding be associated to specific scaling properties of the associated strain field?

The mechanical behavior of disordered cohesive (i.e. non granular) materials, and specifically their approach to final failure, has been widely investigated by the statistical physics community in recent years (e.g. [4-5]) from numerical models such as the random fuse model, the tensorial random spring model or the progressive damage model [6]. Finite size scaling in the power law distributions of avalanche sizes S (defined as the number of broken fibers, bonds or damage events) and energies E have been reported, providing an argument in favor of a critical phase transition interpretation of failure. Recently, from a spatial correlation analysis of damage events as well as a multi-scale analysis of the strain-rate field, Girard et al. [6] reported a divergence of the correlation length as approaching the failure, another strong argument for the critical character of failure.

Following this work, we perform here a coarse graining analysis on the continuous incremental strain field of granular materials at several stages of DEM simulations. This analysis allows a quantitative estimation of the degree of strain localization that take place within the media. Then, the results are interpreted in the framework of statistical physics in order to determine if the macroscopic mechanical features such as the onset of dilatancy or the shear strain softening can be associated to specific scaling laws of the strain-rate field.

2 GRANULAR MODEL

2.1 Microscopic Constitutive laws

The discrete element method involved is one of the most widely used, Molecular Dynamics (MD) [7]. Particles motions are time-discretized with a 3rd order predictor-corrector scheme. All grains interact via linear elastic laws and Coulomb friction when they are in contact: the normal contact force f_n is related to the normal apparent interpenetration δ of the contact as $f_n = k_n \delta$, where k_n is a normal stiffness coefficient ($\delta > 0$ if a contact is present, $\delta = 0$ if there is no contact). The tangential component f_t of the contact force is proportional

to the tangential elastic relative displacement, with a tangential stiffness coefficient k_t. The Coulomb condition $|f_t| \leq \mu f_n$ requires an incremental evaluation of f_t for each time step, which leads to some amount of slip each time one of the equalities $f_t = \mu f_n$ is imposed. In this study, k_n is such that $K = k_n/\sigma_3 = 1000$ [8]. The stiffness ratio is $k_n = k_t = 1$. Granular assemblies are made of two-dimensional rigid circular grains. Their diameters are uniformly distributed between $D_{\min}$ and $D_{max} = 3D_{min}$. Periodic boundary conditions are used [7]. After an isotropic compression without intergranular friction $\mu = 0$, dense samples of initial porosity $n_i = 0.15$ are submitted to a vertical compression with keeping the lateral stress σ_3 constant (biaxial tests). The tests presented in this study consider $\mu = 1$. The vertical constant strain rate $\dot{\varepsilon}_1$ is chosen such that mechanical transformation can be assumed as quasi-static. For that, $\dot{\varepsilon}_1$ is obtained by setting $I = 5.10^{-5}$, where I is the inertial number [8]. Under these considerations, the increment of deformation $\delta\varepsilon_1$ associated to one time step integration is $\delta\varepsilon_1 = 8.5.10^{-9}$.

Figure 1 shows a typical macroscopic stress strain curve obtained on a sample made of 45000 grains. At the beginning of the test, a contracting regime is observed on the volume variation up to an axial strain of about 0.29% corresponding to the onset of dilation: since dense samples are considered here, grains rearrangements in the early stages of deformation are limited and contraction is mainly observed because of an elastic contact description between particles [9]. The inelastic deformation in the contractant regime is due to loss of contact and Coulomb friction between particles. After the peak of contraction, the sample dilates continuously. A maximum shear stress is obtained around 0.65% of macroscopic axial deformation.

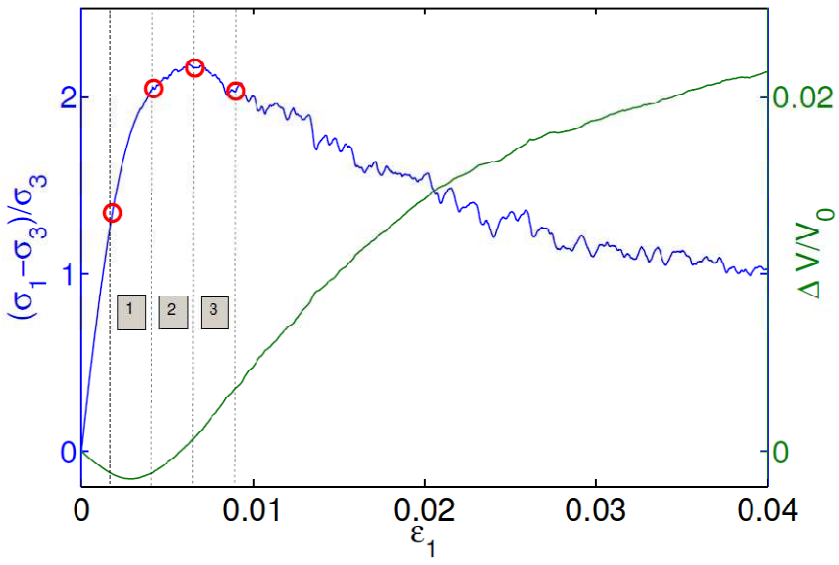

Figure 1: *Macroscopic response of a sample of 45000 grains from 0 to 4% of deformation. The volume deformation is plotted in green and the macroscopic shear stress in blue as a function of axial macroscopic deformation. The onset of dilation is observed around* $\varepsilon_1 = 2.9.10^{-3}$ *and the onset of softening around* $\varepsilon_1 = 6.5.10^{-3}$. *Bold red circles indicate, on the macroscopic shear stress curve, stages where configuration outputs are done. From these 4 configurations, which exhibit 3 interval windows numbered from 1 to 3, associated incremental strain fields are computed and plotted on figure 2. The deformation window size is the same for all the three interval windows and is equal to* $\delta\varepsilon_{large} = 2.4.10^{-3}$.

2.2 Macroscopic shear banding

Many experiments and theoretical works have been conducted in the past in order to describe and understand the onset of macroscopic strain localization within shear bands in geomaterials. Important insights into the mechanics of macroscopic localization were obtained from the continuum analysis of its inception as a bifurcation in the constitutive law [10]. In discrete materials such as soils, the localization of deformation into thin zones of intense shearing is a phenomenon commonly observed [11-14]. It is also assumed that, in the early stages of deformation, homogeneous deformation is observed, while patterns of strain localization appear at some point throughout the test, generally at the peak load or slightly before [11]. It has been reported that these shear bands can form and disappear as deformation proceeds after the peak load [11].

These features are qualitatively observed within our DEM simulations. Figure 2 shows the incremental shear strain fields (computed using equation 2, see section 3) obtained at different stages of the loading by integrating the grains displacements over large deformation windows equal to $\delta\varepsilon_{large} = 2.4.10^{-3}$. We can see that, while heterogeneous, the incremental shear strain field at the beginning of the test (figure 2.1) does not show any clear macroscopic structure. However, as loading goes on, a macroscopic localization materialized by a shear band that spans the entire sample can be distinguished slightly before the peak load (Figure 2.2). Then, these structures essentially perpetuate in time (figure 2.3).

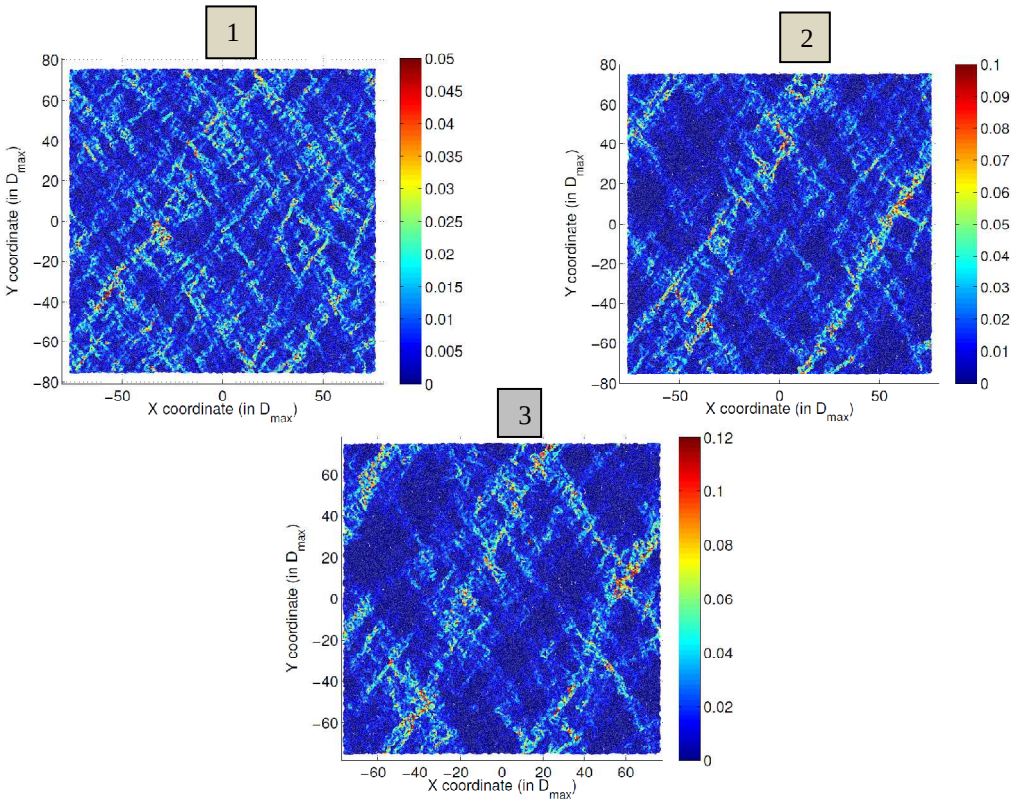

Figure 2: Incremental shear deformation fields from the beginning of the test to the end of the peak load. The shear strain fields are computed by considering deformation windows, of size $\delta\varepsilon_{large} = 2.4.10^{-3}$, materialized on figure 1 (corresponding numbers).

However, by looking more precisely on the incremental strain field, i.e. by considering smaller deformation windows to compute the grains displacements, things become more complex. Associated to the disordered spatial structure of the force network of the initial static granular material [15], intermittent strain heterogeneities emerge from the beginning of the test: patches of variables sizes of intense deformation appear through specific zones, they brutally disappear and the strain field switches to different patterns. Consequently, the mechanical behavior of granular media qualitatively looks highly heterogeneous and intermittent. This intermittency and heterogeneity of the strain field is the key point we aim to quantify in this paper, in order to answer to the following questions: Is this emergence of intermittency and heterogeneity associated to specific scaling laws? Can these processes be connected to final shear banding we observe on figure 2, as a result of the coalescence and interaction of structured localized zones?

To answer to these fundamental questions, we perform a coarse graining analysis on the strain rate field.

3 COARSE GRAINING ANALYSIS

Incremental strain are computed over a broad range of spatial scales at different stages of macroscopic deformation from a coarse graining analysis similar to that of Marsan et al. [16]. The configurations are saved for each simulation with a constant deformation interval $\delta\varepsilon_w$ chosen to be equal to 5.10^{-6}. This choice for $\delta\varepsilon_w$ is justified in section 4.3. The increments (u_i, v_i) of displacements of each particle i are computed from the difference in the particle positions (x_i, y_i) between two successive configurations. Then, a mesh triangulation is performed on the grains centers, and the spatial derivatives $\partial u/\partial x$, $\partial u/\partial y$, $\partial v/\partial x$ and $\partial v/\partial y$ of the incremental displacements associated to each element of the mesh are computed following a contour integral.

In the following, we focus on two invariants of the incremental strain tensor:

- the divergence

$$\delta\varepsilon_{\mathrm{v}} = \delta\varepsilon_1 + \delta\varepsilon_2 = \frac{\partial u}{\partial x} + \frac{\delta v}{\delta y} \tag{1}$$

- the shear

$$\delta\gamma = \delta\varepsilon_1 - \delta\varepsilon_2 = \sqrt{\left(\frac{\partial v}{\partial y} - \frac{\partial u}{\partial x}\right)^2 + \left(\frac{\partial v}{\partial x} - \frac{\partial u}{\partial y}\right)^2} \tag{2}$$

where $\delta\varepsilon_1$ and $\delta\varepsilon_2$ are the principal components of the incremental strain tensor.
The scaling properties of the incremental divergence and shear fields are then explored from a coarse graining analysis [6,16].

First, deformation at the micro scale, i.e. the mesh scale, is computed. Then, at larger spatial scales, deformation is obtained by splitting the sample into square cells of size ranging from the micro scale to the macro scale (the simulation box). Consider a square cell of width W at a certain location within the sample. We find all the element centers of the mesh that lie inside the box and compute the average spatial derivatives $\partial u/\partial x$,.. over all the corresponding elements,

where the contribution of each element is weighted by its area. From these gradients, thus averaged at the scale W, we compute the incremental strain invariants $\delta\varepsilon_v$ and $\delta\gamma$ following (1) and (2). Assuming scaling isotropy, we define the effective spatial scale L of the cell as the square root of the area covered by the elements (which is close but not exactly equal to W). This procedure is repeated for all the other cells of the same width W that cover the sample (no overlap is considered here). Average values $< |\delta\varepsilon_v| >$ and $< \delta\gamma >$ are computed by averaging the incremental divergent strain modulus $|\delta\varepsilon_v|$ and the incremental shear strain $\delta\gamma$ over all the cells of the same width. W is logarithmically binned starting from W_{macro} i.e. W is iteratively equal to W_{macro}, $W_{macro}/2$, $W_{macro}/4$, etc… (Figure 3).

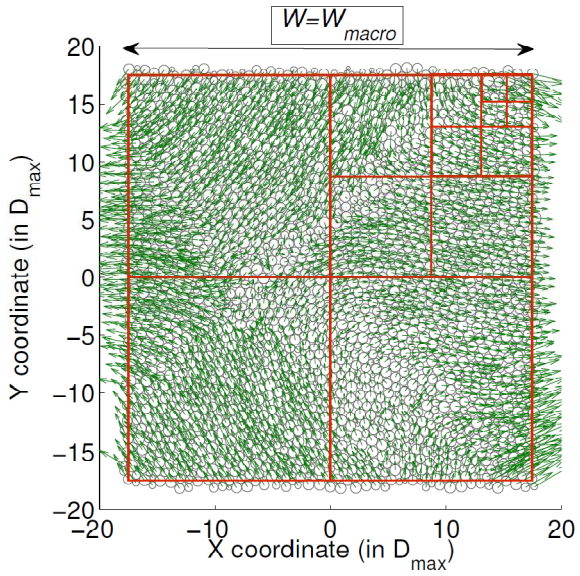

Figure 3: Illustration of the coarse graining method on a sample of 2500 grains. The green arrows show the displacement vector for each grain between the two successive configurations taken near the peak load. The red boxes show the areas considered to compute the incremental strains at scales ranging from macro to micro scale.

4 RESULTS

In the following, all the results are averaged over coarse graining analyses conducted on 50 simulations of 10000 grains. Similar results were obtained with simulations of 45000 grain. From one simulation to another, the only changing sample property is the initial random organization of the grains in space, inducing changes within the force network disorder.

4.1 Contractancy

Figure 4 plots the average of the incremental divergent strain modulus $< |\delta\varepsilon_v| >$ as a function of scale L in the early stages of biaxial testing, up to dilatancy (Figure 4).
At the early stages of deformation ($\varepsilon_1 = 1.1.10^{-3}$), black curve on Figure 4(b), $< |\delta\varepsilon_v| >$ does not vary with L, which means that the incremental divergent deformation is homogeneously scattered throughout the sample. As macroscopic deformation proceeds, a decrease of $< |\delta\varepsilon_v| >$ with L is observed at small scales while, for L-values larger than a crossover scale denoted L_v^*, a plateau is observed. This means that, for $L << L_v^*$, the incremental divergent deformation is heterogeneous while homogeneity can only be assumed for $L >> L_v^*$. Finally, at the point corresponding to the maximum of contraction (i.e. the onset of macroscopic dilation), a power law scaling over the entire range of scales is observed on $< |\delta\varepsilon_v| >$: the divergent incremental deformation is at that point highly heterogeneous, from the grain scale to the macroscopic scale, and no characteristic size appears.

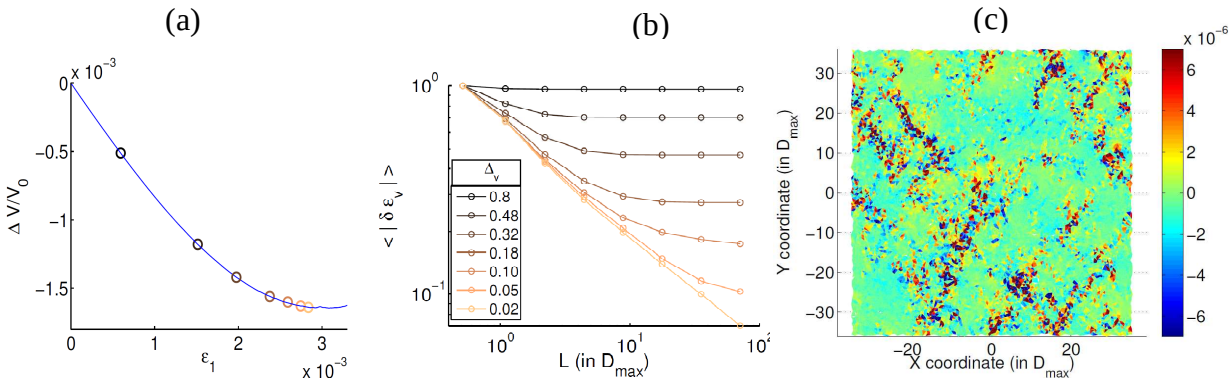

Figure 4: Multi-scale evolution of (b) the incremental divergent deformation from the beginning of the test to the onset of macroscopic dilation. The curves are normalized by the average incremental divergent deformation computed at the mesh scale. The bold circles on (a) indicate on the macroscopic volume variation curve the locations where two successive configurations are taken to perform the coarse graining analysis. Colors convention is the same on the two plots. (c) Incremental divergent deformation field at the peak of contraction. All the calculations are done using $\delta\varepsilon_w = 5.10^{-6}$.

These results suggest a progressive structuring of the divergence rate field as approaching the peak of contraction, where the crossover scale L^*, interpreted here as a correlation length [6], diverges. To test this hypothesis, we define a control parameter Δ_v as follows:

$$\Delta_v = \frac{\varepsilon_1^{cv} - \varepsilon_1}{\varepsilon_1^{cv}} \quad (3)$$

where $\varepsilon_1^{cv} = 2.9.10^{-3}$ is the value of axial deformation ε_1 at the peak of contraction. Thus, Δ_v is equal to 0 at $\varepsilon_1 = \varepsilon_1^{cv}$, and the mean incremental divergent strain modulus can be expressed as

$$< |\delta\varepsilon_v| > (L, \Delta_v) \sim L^{-\rho_v} H_v\left(\frac{L}{L_v^*}\right) \quad (4)$$

where H_v describes the crossover: it is thus constrained by $H_v\left(\frac{L}{L_v^*}\right) \sim$ const for $L \ll L_v^*$ and $H_v\left(\frac{L}{L_v^*}\right) \sim L_v^{\rho_v}$ for $L \gg L_v^*$.

We further hypothesize that L_v^* diverges as approaching ε_1^{cv} as $L_v^* \sim \Delta^{-\nu_v}$, and we estimate the exponent values from a data collapse analysis (Figure 5).

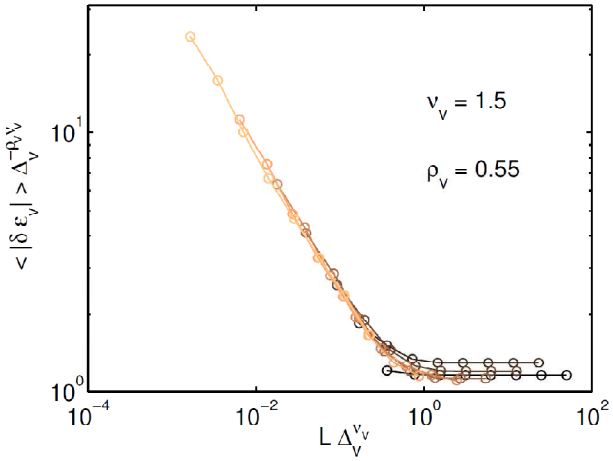

Figure 5: Data collapse analysis of the average divergence rate. The values used for the exponents are ρ_v = 0.55 ± 0.05 and ν_v = 1.5 ± 0.1.

ρ_v = 0.55 ± 0.05 and ν_v = 1.5 ± 0.1 allow the best collapse.

We tested the significance of this observation by randomly reshuffling the spatial derivatives of the incremental displacements in space. Doing this, the coarse graining analysis shows no power law trend. Hence, the observed power law scaling of $< |\delta\varepsilon_v| >$ with L at the peak of contraction is the result of the spatial correlations present in the divergent deformation field and can be related to the spatial structure of the deformation field. The correlation length L_v^* is small at the onset of macroscopic deformation, and represents in this case the size of a representative elementary "volume" (REV). On the other hand, the power law divergence of the correlation length L_v^* at $\varepsilon_1 = \varepsilon_1^{cv}$ leads us to conclude that the peak of contraction plays the role of a critical point with respect to the divergent deformation field in granular materials. On the contrary, at that stage, no scaling is observed for the incremental shear deformation field $< \delta\gamma >$.

4.2 Shear banding

In order to see if a similar "critical-like" behavior can be associated to macroscopic shear faulting and/or the onset of macroscopic softening, we performed a coarse graining analysis on the incremental shear deformation $< \delta\gamma >$. Strain configurations are selected in this case with respect to the loading curve τ versus ε_1 (Figure 6(a)), where $\tau = (\sigma_1 - \sigma_3)/\sigma_3$ is the deviatoric stress. Looking at $< \delta\gamma >$ versus L on Figure 6(c), a similar behavior with the one presented in the previous section on the divergent strain field is observed: a rather homogeneous incremental shear strain field (i.e. a small associated correlation length) is observed in the early stages of deformation, and a power law scaling is building up as ε_1 increases.

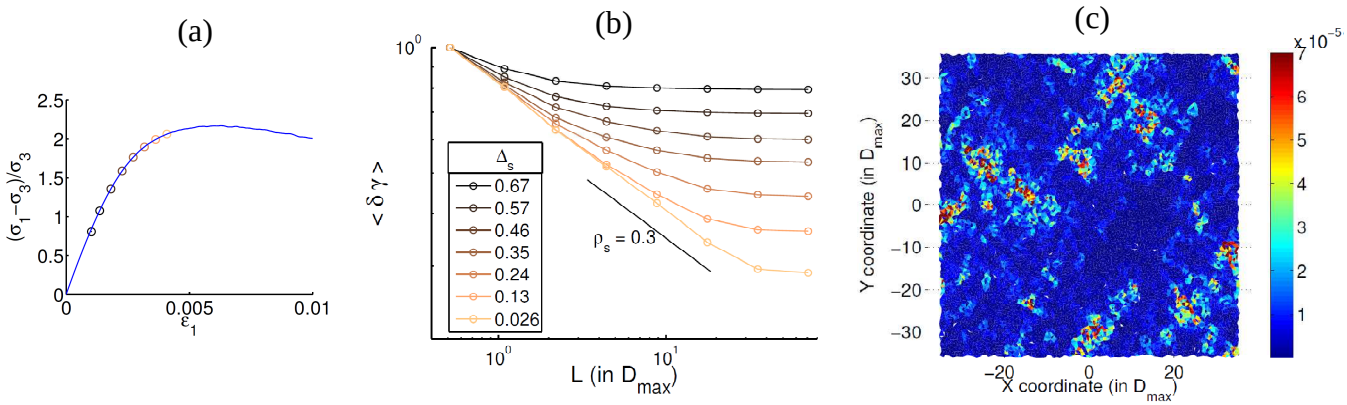

Figure 6: Multi-scale evolution of (b) the incremental shear deformation from the beginning of the test to $\varepsilon_1^{sat} = 4.1.10^{-3}$ i.e. slightly before the peak load. The bold circles on (a) indicate on the loading curve the locations where two successive configurations are taken to perform the coarse graining analysis. Colors are respected on the three plots. (c) Incremental shear field at $\varepsilon_1^{cs} = 4.2.10^{-3}$. All the computations are done by considering $\delta\varepsilon_w = 5.10^{-6}$.

The power law decrease of $< \delta\gamma >$ with L at small scales shows an exponent ρ_s equal to 0.3. However, unlike what was observed for the incremental divergent deformation in the preceding section, from $\varepsilon_1^{sat} = 4.1.10^{-3}$, the correlation length L_s^* seems to saturate at a value $L_{sat}^* \approx 30D_{max}$. In other words, power law scaling never develops over the entire scale range in the present case. We checked that L_{sat}^* does not depend on the size of the system considered, i.e. does not result from a finite size effect.

Nevertheless, we verified that a scaling similar to equation (4) well describes the results of figure 6b and the corresponding increase of L_s^*, up to the limiting value L_{sat}^*. To do so, we define, following equation (3), a second control parameter Δ_s equal to 0 at an axial deformation $\varepsilon_1 = \varepsilon_1^{cs}$, and express the average incremental shear strain as:

$$< \delta\gamma > (L, \Delta_s) \sim L^{-\rho_s} H_s\left(\frac{L}{L_s^*}\right) \qquad (5)$$

where H_s describes the crossover as in previous section. At this stage, ε_1^{cs} is unknown but is necessarily larger than ε_1^{sat}.

We then hypothesize that L_s^* grows as $L_s^* \sim \Delta_s^{-\nu_s}$, and we estimate the exponent values as well as the axial strain ε_1^{cs} from a data collapse analysis (Figure 6).
$\varepsilon_1^{cs} = 4.2.10^{-3}$, $\rho_s = 0.3 \pm 0.05$ and $\nu_s = 2.0 \pm 0.2$ allow the best collapse.

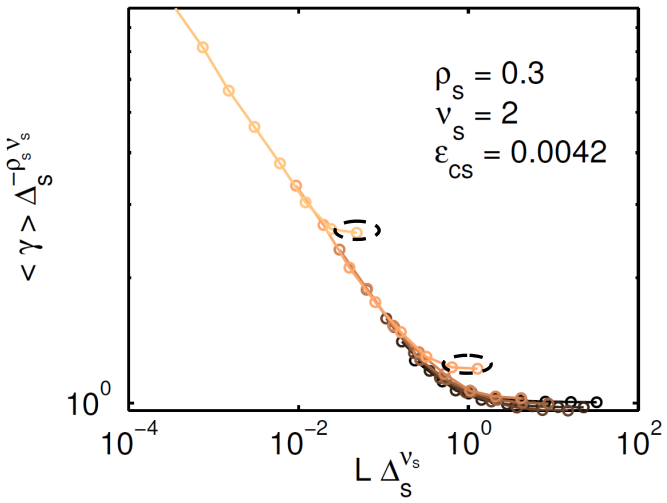

Figure 6: Data collapse analysis realized on the average shear deformation rate. The values used for the exponents are ρ_s = 0.3 ± 0.05 and ν_s = 2.0 ± 0.2. The black bold circles highlight the deviation from power law scaling of the correlation length L_s^* for $\varepsilon_1 > \boldsymbol{\varepsilon_1^{sat}}$.

This collapse works well for $\Delta_s \geq 0.15$ i.e. for values of axial deformation ε_1 lower than $3.6.10^{-3}$, providing that the choice of $\varepsilon_1^{cs} = 4.2.10^{-3}$ is convenient. However, when axial deformation proceeds further towards ε_1^{cs} (i.e. $\varepsilon_1 > 3.6.10^{-3}$), a deviation from the scaling form (5) is observed (black dashed circles on Figure 6), as the result of the saturation of the correlation length. This saturation indicates that the divergence is not complete. Consequently, the shear deformation rate field seems to organize with respect to a specific level of applied strain $\varepsilon_1^{cs} = 4.2.10^{-3}$, although this evolution is stopped before to spread over the full range of spatial scales, near $\varepsilon_1 = 3.6.10^{-3}$.

It is interesting to note that this axial strain $\varepsilon_1^{cs} = 4.2.10^{-3}$ corresponds to a deformation stage slightly before the peak load, corresponding to the point at which the formation of a macroscopic shear band is qualitatively reported in experiments [11] and also in our DEM model (Figure 2), as the shear strain field #2 plotted on figure 2, computed over an axial strain window of $\delta\varepsilon_{large} = 2.4.10^{-3}$, exactly starts at $\varepsilon_1^{cs} = 4.2.10^{-3}$. When calculated over a much smaller strain window of 5.10^{-6}, the incremental shear strain field at ε_1^{cs} (figure 6c) shows strain clusters, however not organized into a macroscopic shear band spanning the entire sample. Unlike the shear bands of figure 2, these strain clusters do not perpetúate and are instead highly intermittent (not shown). Therefore, the structuration of the shear strain seems to be dependent on the size of the strain window considered.

4.3 Strain window size dependency

The calculations shown in section 4.2 were performed using a deformation window $\delta\varepsilon_w$ of 5.10^{-6} between two successive configurations. While considering larger deformation window sizes does not affect the dependence of $< |\delta\varepsilon_v| >$ with L (similar results than the one shown in section 4.1 are reported), this is not the case for $< \delta\gamma >$. Because highly intermittent in time in the vicinity of the peak load, the scaling properties of the incremental shear field are largely affected by the deformation window size, i.e. the value of $\delta\varepsilon_w$ considered to compute the grains displacements. Figure 7 plots the results of the coarse graining analysis performed around $\varepsilon_1^{cs} = 4.2.10^{-3}$ for several values of $\delta\varepsilon_w$, ranging from 5.10^{-6} to $2.4.10^{-3}$.

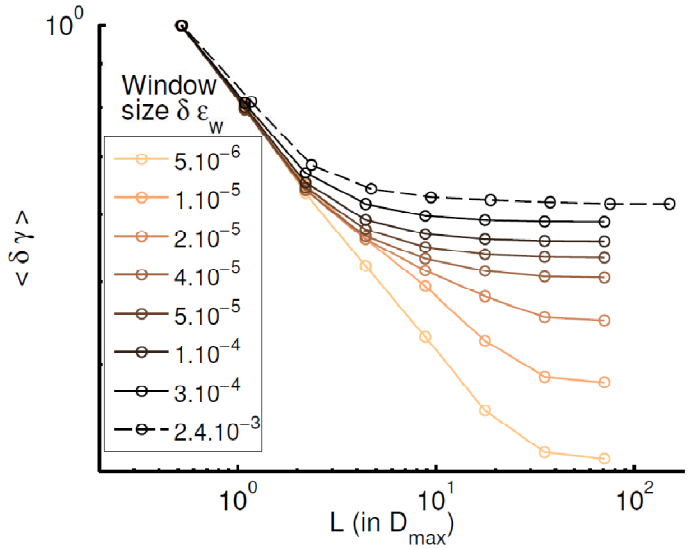

Figure 7: Influence of the deformation window size $\delta\varepsilon_w$ on the scaling properties of the deformation field at $\varepsilon_1^{cs} = 4.2.10^{-3}$. Colored continuous lines are computed by considering deformation windows centered at ε_1^{cs}. The black dashed line results from a coarse graining analysis conducted on the incremental shear strain field #2 of Figure 2, obtained with a simulation of 45000 particles.

The departure from power law behavior at large spatial scales L as $\delta\varepsilon_w$ increases is obvious on this plot. It has been checked that the multi-scale properties of the shear rate deformation field are not affected when considering values of $\delta\varepsilon_w$ five times smaller than 5.10^{-6}. This means that, at $\varepsilon_1^{cs} = 4.2.10^{-3}$ and for small deformation window sizes (inferior to 5.10^{-5}), the shear strain field is characterized by large correlation length values, up to $30D_{max}$. By opposition, small correlation lengths of about $3D_{max}$ clearly appear when considering large deformation window sizes, i.e. greater than 2.10^{-5}. These small correlation lengths observed at large deformation windows seem to be robust, since the cross-over remains approximately the same for values of $\delta\varepsilon_w$ varying of 2 orders of magnitudes, from 5.10^{-5} to $2.4.10^{-3}$.
Thus, two distinct behaviors can be outlined:

- Large correlation lengths are reported at small strain window sizes. This point out the fact that elastic interactions between particles allow the system to communicate via long range interactions. The associated spatial deformation field pattern is materialized by patches of intense shearing, highly intermittent in space and time.

- Small correlation lengths are reported at large strain window sizes. This means that the intermittent character of the shear deformation field associated to the development of self affine structures observed at small strain window sizes within the deformation field gives rise to the observation of a macroscopic shear band at large enough strain window sizes. The correlation length given by the coarse graining analysis is associated to the width of the macroscopic shear band, here equal to $3D_{max}$.

5. CONCLUSION

We have shown that, during compressive loading, spatial correlations associated to the coalescence and interaction of structured localized zones take place within the deformation field of frictional granular materials. The associated correlation length can be extracted from a coarse graining analysis. Specific scaling properties of the divergent and shear strain field, which behave separately, are associated to macroscopic evidences:

- The divergence of the correlation length associated to the incremental divergent strain field modulus as approaching the onset of macroscopic dilation is reported. This means that the peak of contraction, located at $\varepsilon_1^{cv} = 2.95.10^{-3}$, plays the role of a critical point with respect to the divergent deformation field.
- The increase of the correlation length within the incremental shear strain field is reported until $\varepsilon_1 = 4.1.10^{-3}$is reached, where a remaining saturation is observed at large scales on the power law scaling. We have shown that the shear deformation field organizes itself with respect to a specific level of applied strain $\varepsilon_1^{cs} = 4.2.10^{-3}$, located slightly before the peak load. We argue that this point corresponds to the onset of macroscopic shear banding.

Finally, because highly intermittent in time and space, the shear strain field shows scaling properties that are largely controlled by the strain window size considered. Large spatial correlations are observed at small strain windows, while small spatial correlations, equal to the width of the macroscopic shear band when looking after $\varepsilon_1^{cs} = 4.2.10^{-3}$, are observed at large strain windows.

A remaining question is how such intermittency observed at very small time scales within the deformation field, meaning that the deformation field loses its memory rapidly, leads to the development of perennial structures materialized by a macroscopic shear band at large time scale.

REFERENCES

[1] Radjai, F. and Roux, S. Turbulent-like Fluctuations in Quasistatic Flow of Granular Media, *Phys. Rev. Lett.*, (2002) **89**:064302.
[2] Liu, C.-h., Nagel, S. R., Schecter, D.A., Coppersmith, S.N., Majumdar, S., Narayan and O., Witten, T.A. Force Fluctuations in Bead Packs. *Science* (1995) **269**:513-515.
[3] Staron, L., Radjai, F. and Vilotte, J.P. Multi-scale analysis of the stress state in a granular slope in transition to failure. *Eur. Phys. J. E*. (2005) **18**:311-320.
[4] Herrmann, H.J. and Roux, S. *Statistical Models for the Fracture of Disordered Media*. North-Holland (1990)
[5] Alava, M. J., Nukala, P.K. and Zapperi, S. Statistical models of fracture. *Advances in*

Physics (2006) **55**:349-479.
[6] Girard, L, Amitrano, D. and Weiss, J., Failure as a critical phenomenon in a progressive damage model. *J. Stat. Mech.* (2010) P01013.
[7] Radjai, F. and Dubois, F. *Discrete Numerical Modeling of Granular Materials.* John Wiley & Sons (2011).
[8] Combe, G. and Roux, J.-N. Discrete numerical simulation, quasistatic deformation and the origins of strain in granular materials. *3ème Symposium International sur le Comportement des sols et des roches tendres*. Lyon (2003) In di Benedetto et al., pp 1071-1078.
[9] Roux, J.N. and Combe, G. How granular materials deform in quasistatic conditions. *IUTAM-ISIMM Symposium on Mathematical Modeling and Physical Instances of Granular Flows, AIP Conference Proceedings*, (2010) **1227:**260-270.
[10] Rudnicki, J.W. and Rice, J.R. Conditions for the localization of deformation in pressure-sensitive dilatant materials, *J. Mech. Phys. Sol.* (1975) **23**:371-394.
[11] Desrues, J. and Viggiani, G. Strain localization in sand: an overview of the experimental results obtained in Grenoble using stereophotogrammetry. *Int. J. Num. An. Meth. Geomech.*(2004) **28**:279-321.
[12] Hall S., Muir Wood, D., Ibraim E., Viggiani G. Localised deformation patterning in 2D granular materials revealed by digital image correlation, *Granular Matter* (2010) **12**:1-14.
[13] Calvetti F., Combe G., Lanier J. Experimental micromechanical analysis of a 2D granular material : relation between structure evolution and loading path, *Mechanics of Cohesive Frictional Materials* (1997) **2**:121-163
[14] K. Szarf, G. Combe, P. Villard Polygons vs. clumps of discs: a numerical study of the influence of grain shape on the mechanical behaviour of granular materials. *Powder Technology* (2011) **208**:279-288.
[15] Ostojic, S., Somfai E. and Nienhuis, B. Scale invariance and universality of force networks in static granular matter, *Nature* (2006) **439**:828-830.
[16] Marsan, D., Stern, H., Lindsay, R. and Weiss, J. Scale Dependence and Localization of the Deformation of Arctic Sea Ice. *Phys. Rev. Lett.* (2004) **93**:178501.
[17] Radjai, F. and Richefeu, V. Contact dynamics as a nonsmooth discrete element method, *Mech. Mat.* (2009) **41**:715-728.